

**Relativistic recoil, electron-correlation, and QED effects on the
 $2p_j - 2s$ transition energies in Li-like ions**

Y. S. Kozhedub¹, A. V. Volotka^{1,2}, A. N. Artemyev³, D. A. Glazov¹,
G. Plunien², V. M. Shabaev¹, I. I. Tupitsyn¹, and Th. Stöhlker^{3,4}

¹ *Department of Physics,
St. Petersburg State University,
Oulianovskaya 1, Petrodvorets,
St. Petersburg 198504, Russia*

² *Institut für Theoretische Physik,
Technische Universität Dresden,
Mommensenstraße 13,
D-01062 Dresden, Germany*

³ *Physikalisches Institut,
Universität Heidelberg, Philosophenweg 12,
D-69120 Heidelberg, Germany*

⁴ *GSI Helmholtzzentrum für Schwerionenforschung GmbH,
Planckstrasse 1, D-64291 Darmstadt, Germany*

Abstract

The relativistic nuclear recoil, higher-order interelectronic-interaction, and screened QED corrections to the transition energies in Li-like ions are evaluated. The calculation of the relativistic recoil effect is performed to all orders in $1/Z$. The interelectronic-interaction correction to the transition energies beyond the two-photon exchange level is evaluated to all orders in $1/Z$ within the Breit approximation. The evaluation is carried out employing the large-scale configuration-interaction Dirac-Fock-Sturm method. The rigorous calculation of the complete gauge invariant sets of the screened self-energy and vacuum-polarization diagrams is performed utilizing a local screening potential as the zeroth-order approximation. The theoretical predictions for the $2p_j - 2s$ transition energies are compiled and compared with available experimental data in the range of the nuclear charge number $Z = 10 - 60$.

PACS numbers: 31.30.J, 31.30.Gs

I. INTRODUCTION

High-precision spectroscopy of Li-like ions continues to be of interest both theoretically and experimentally. On the one hand such ions are among the simplest few-electron systems that can be theoretically described with high accuracy, on the other hand high precision measurements are also available. Investigations of such systems enable precision tests of quantum electrodynamics (QED) at strong fields, as well as studying various nuclear properties probed by the atomic structure. During the last decades significant theoretical efforts were undertaken to evaluate various contributions to the energy levels in high- Z Li-like ions [1–16]. However, further improvements in theoretical calculations are required in order to meet the high level of the experimental accuracy [17–26].

This work is devoted to high precision calculations of the $2p_j - 2s$ transition energies in middle- Z Li-like ions. As was noticed in Ref. [13], the leading sources of theoretical uncertainty originate from the relativistic recoil and higher-order screened QED corrections. Therefore, the present paper is mainly focused on evaluation of these corrections. The paper is organized as follows: Sec. II is devoted to the calculation of the relativistic nuclear recoil effect employing the large-scale configuration-interaction Dirac-Fock-Sturm method (CI-DFS). The method used for the calculation of the higher-order (in $1/Z$) relativistic recoil corrections allows us also to obtain accurate numerical values for the interelectronic-interaction contributions to the transition energies within the Breit approximation. In Sec. III these results are combined with the rigorous QED calculation of the one- and two-photon exchange contributions to obtain the higher-order electron-electron interaction corrections to the transition energies with the same accuracy level as in Ref. [13]. The calculation of the screened QED corrections is presented in Sec. IV. A local screening potential is included in the zeroth-order Hamiltonian. Then, the first and second-order diagrams representing the screened self-energy (SE) and vacuum-polarization (VP) corrections are rigorously evaluated. In the last section, we compile all the contributions to get the most accurate theoretical predictions for the $2p_{1/2} - 2s$ and $2p_{3/2} - 2s$ transition energies of Li-like ions in the range of the nuclear charge number $Z = 10 - 60$ and compare them with experimental data available.

Relativistic units ($\hbar = 1$, $c = 1$, $m = 1$) and the Heaviside charge unit [$\alpha = e^2/(4\pi)$, $e < 0$] are used throughout the paper.

II. RELATIVISTIC THEORY OF THE NUCLEAR RECOIL EFFECT

Since the electron mass is small compared to the nucleus mass, most of the contributions to the binding energies can be evaluated within the infinite nuclear mass approximation. Taking into account a finite nuclear mass shifts the energies. This is so called nuclear recoil effect. Since this effect is different for different isotopes, it also results in an isotope shift of the energy levels. Generally, the isotope shift arises as a sum of the finite nuclear mass effect (mass shift) and a non-zero nuclear size effect (field shift). In this section we focus on calculations of the mass shift in Li-like ions.

A. Basic formulas

In the nonrelativistic theory the mass shift (MS) is usually represented as a sum of the normal mass shift (NMS) and the specific mass shift (SMS), $H_M^{(\text{nonrel})} = H_{NMS} + H_{SMS}$, where [27]

$$\begin{aligned} H_{NMS} &= \frac{1}{2M} \sum_i \mathbf{p}_i^2, \\ H_{SMS} &= \frac{1}{2M} \sum_{i \neq j} \mathbf{p}_i \cdot \mathbf{p}_j. \end{aligned} \quad (1)$$

Here, \mathbf{p}_i is the electron momentum operator and M is the nuclear mass.

A rigorous relativistic theory of the mass shift can be formulated only in the framework of QED. Such a theory was formulated in Refs. [28, 29] (see also Refs. [30, 31] and references therein), where the complete αZ -dependent formulas for the recoil correction to the atomic energy levels to first order in m/M were derived. Within the Breit approximation this theory leads to the following many-body relativistic MS Hamiltonian:

$$H_M = \frac{1}{2M} \sum_{i,j} \left\{ \mathbf{p}_i \cdot \mathbf{p}_j - \frac{\alpha Z}{r_i} \left[\boldsymbol{\alpha}_i + \frac{(\boldsymbol{\alpha}_i \cdot \mathbf{r}_i) \mathbf{r}_i}{r_i^2} \right] \cdot \mathbf{p}_j \right\}, \quad (2)$$

where $\boldsymbol{\alpha}$ is a vector incorporating the Dirac matrices. An independent derivation of Hamiltonian (2) was presented in Ref. [32]. As follows from expression (2), the lowest-order relativistic correction to the one-electron mass shift operator is given by

$$H_{RNMS} = -\frac{1}{2M} \sum_i \frac{\alpha Z}{r_i} \left[\boldsymbol{\alpha}_i + \frac{(\boldsymbol{\alpha}_i \cdot \mathbf{r}_i) \mathbf{r}_i}{r_i^2} \right] \cdot \mathbf{p}_i, \quad (3)$$

where ‘‘RNMS’’ stays for the relativistic NMS. The corresponding two-electron correction is

$$H_{\text{RSMS}} = -\frac{1}{2M} \sum_{i \neq j} \frac{\alpha Z}{r_i} \left[\boldsymbol{\alpha}_i + \frac{(\boldsymbol{\alpha}_i \cdot \mathbf{r}_i) \mathbf{r}_i}{r_i^2} \right] \cdot \mathbf{p}_j, \quad (4)$$

where ‘‘RSMS’’ denotes the relativistic SMS.

The recoil correction to a given atomic state to first order in m/M is obtained as the expectation value of H_M on the Dirac wave function (here and in what follows, the Dirac wave functions are the eigenvectors of the Dirac-Coulomb-Breit Hamiltonian). In Ref. [33] the Hamiltonian (2) was employed to calculate the $(\alpha Z)^4 m/M$ corrections to the energy levels in He- and Li-like ions to zeroth order in $1/Z$. Later in Refs. [34, 35], this Hamiltonian was used to evaluate the relativistic recoil effect in low- and middle- Z ions and atoms to all orders in $1/Z$.

The recoil correction of the first order in m/M is conveniently expressed in terms of the constant K defined by

$$\Delta E = \langle \psi | H_M | \psi \rangle \equiv K/M, \quad (5)$$

where $|\psi\rangle$ is the eigenvector of the Dirac-Coulomb-Breit Hamiltonian. With this constant, the mass isotope shift for two different isotopes with nuclear masses M_1 and M_2 can be written as $\delta E = K \left(\frac{1}{M_1} - \frac{1}{M_2} \right)$.

The recoil correction which is beyond the Breit approximation (2) is referred to a QED recoil effect. This effect has to be also taken into account, especially for high- Z ions. For H- and Li-like ions the QED recoil corrections have been calculated to all orders in αZ and to zeroth order in $1/Z$ in Refs. [36, 37]. In what follows, we focus on the calculations of the coefficient K to all orders in $1/Z$ for the $2p_j - 2s$ transitions in a wide range of Li-like ions. We investigate relative contributions of the relativistic and QED corrections to the total recoil effect and the influence of the electron correlations on the recoil effect.

B. Method of calculation

Expectation values of the MS operator (2) are very sensitive to the electron correlations. In the present investigation the large-scale configuration-interaction (CI) Dirac-Fock-Sturm (DFS) method was employed to solve the Dirac-Coulomb-Breit equation with high accuracy. This method was developed by Tupitsyn and partially presented in Ref. [38]. It was

successfully used for calculations of the recoil effect in Refs. [14, 34]. The MS is calculated as the expectation value of the recoil operator with the many-electron Dirac wave function. Additionally, we apply an alternative approach which consists in adding the operator H_M (2) to the many-electron Hamiltonian H with an arbitrary coefficient λ

$$H(\lambda) = H + \lambda H_M \quad (6)$$

and evaluating the MS by

$$\Delta E = \left. \frac{d}{d\lambda} E(\lambda) \right|_{\lambda=0}. \quad (7)$$

Here the derivative is determined numerically and λ is chosen obeying the numerical stability and smallness of the nonlinear terms. We have reformulated the CI-DFS method to adopt the alternative scheme and independently evaluated the normal and specific parts of the MS by both methods.

C. Results of the calculations and discussion

Here we examine our calculations of the mass shift coefficient K in Li-like ions and compare them with the related results obtained by other authors. In Tables I, II, III, and IV we present numerical results for the coefficient K calculated for the $2p_{1/2} - 2s$ and $2p_{3/2} - 2s$ transitions in lithium, Li-like zinc, neodymium, and uranium, respectively. The first line shows the contribution obtained employing the MS operator (2). The entries labeled “NMS”, “SMS”, “RNMS” and “RSMS” represent the corresponding contributions of the mass shift operators. Since the expectation values of the NMS and SMS operators are evaluated with the Dirac wave functions, the values denoted by NMS and SMS in the tables partly contain the relativistic contributions. The values marked by “nr” show the nonrelativistic values of the corresponding contributions, obtained within the same computing procedure but with a 1000-times increased value of the speed of light (in atomic units). We have verified this nonrelativistic limit by comparing our values with the results of the fully nonrelativistic method based on the Schrödinger Hamiltonian and on the same calculation scheme. The values have exactly coincided with each other for all the ions under consideration. To demonstrate the importance of the electron-electron interaction effects we present also the related results obtained with the hydrogenlike wave functions. These values are marked as “hyd” in the tables. Obviously, the CI-DFS approach is not the best for very low- Z Li-

Table I. Individual contributions to the mass shift coefficient K (GHz·amu) for the $2p_{1/2} - 2s$ and $2p_{3/2} - 2s$ transitions in lithium ($Z=3$).

Subset	$2p_{1/2} - 2s$	$2p_{3/2} - 2s$	Ref.	
MS operator	-443.81(20)	-443.82(20)		
	-443.86 ^{nr}	-443.86 ^{nr}		
	-2534.48 ^{hyd}	-2535.12 ^{hyd}		
	NMS	-245.48	-245.49	
	SMS	-198.78	-198.77	
	-198.73 ^{nr}	-198.73 ^{nr}		
	-198.920(2) ^{nr}	-198.920(2) ^{nr}	[39–41]	
	-198.8 ^{nr}	-198.8 ^{nr}	[42]	
RNMS	0.33	0.38		
RSMS	0.12	0.06		
QED	-0.08(3)	-0.08(3)		
1-el QED	-0.08	-0.08		
2-el QED	0.00	0.00		
Total theory	-443.9(2)	-443.9(2)		
	-444.086	-444.103	[43, 44]	
	-447(12)	-447(12)	[35]	
Experiment*	-444.09(3)		[45]	
	-444.04(4)	-444.06(4)	[46]	

* The experimental values include also terms of higher orders in m/M .

like systems. Most accurate results for lithium are presently obtained utilizing variational solutions of the three-body Schrödinger problem and accounting for the relativistic and QED corrections within the αZ expansion [43, 44]. We use these results to estimate the residual correlation effects in our calculations. Analyzing the convergence of the calculated atomic properties as a function of the configuration basis set, the difference between the results obtained by two alternative methods described above, and the deviation of our nonrelativistic

Table II. Individual contributions to the mass shift coefficient K (GHz·amu) for the $2p_{1/2} - 2s$ and $2p_{3/2} - 2s$ transitions in Li-like zinc ($Z=30$).

Subset	$2p_{1/2} - 2s$	$2p_{3/2} - 2s$	Ref.
MS operator	-224600(3)	-230073(3)	
	-230161 ^{nr}	-230161 ^{nr}	
	-246954 ^{hyd}	-253951 ^{hyd}	
NMS	-21862.0	-34139.7	
SMS	-235922.0	-225509.0	
RNMS	13807.8	22890.0	
RSMS	19377.1	6685.8	
QED	-591(20)×10	-560(20)×10	
1-el QED	-5411	-5504	
2-el QED	-497	-98	
Total theory	-23051(20)×10	-23568(20)×10	

SMS values from the related results by other nonrelativistic calculations, we estimate an uncertainty associated with the electron correlation as 0.05% for lithium, 0.002% for Li-like boron and much less for ions with larger nuclear charge numbers.

One-electron and two-electron QED recoil corrections were calculated in accordance with our previous works [36, 37, 47]. The evaluation is performed for extended nuclei within the approximation of noninteracting electrons. The electron-electron interaction is suppressed by a factor $1/Z$, therefore we estimate the uncertainty of the QED recoil contribution multiplying it by $1/Z$.

As one can see, in the case of Li our values agree well with the previous theoretical predictions [35, 39–44] as well as with the experimental data [45, 46].

In Fig. 1 we plot the individual contributions to the MS coefficient K for the $2p_{1/2} - 2s$ and $2p_{3/2} - 2s$ transitions in Li-like ions. The dotted line indicates the relative contribution of the electron-electron interaction; the dashed line represents the relativistic correction; and the dashed-dotted line stands for the QED part of the coefficient. We observe that for low- Z ions it is extremely important to include the electron-electron interaction effects.

Table III. Individual contributions to the mass shift coefficient K (GHz·amu) for the $2p_{1/2} - 2s$ and $2p_{3/2} - 2s$ transitions in Li-like neodymium ($Z=60$).

Subset	$2p_{1/2} - 2s$	$2p_{3/2} - 2s$	Ref.
MS operator	-834508(25)	-962662(25)	
	-967156 ^{nr}	-967156 ^{nr}	
	-868746 ^{hyd}	-1014056 ^{hyd}	
NMS	-339895	-625227	
SMS	-1227059	-998772	
RNMS	323477	539494	
RSMS	408969	121843	
QED	-2133(35)×10 ²	-1958(35)×10 ²	
1-el QED	-175010	-188435	
2-el QED	-38285	-7332	
Total theory	-10478(35)×10 ²	-11584(35)×10 ²	

For middle- Z ions all parts are equally important. For high- Z region the QED and relativistic contributions become dominant. It is interesting to note that for the high Z the QED contribution is larger than the relativistic one. One can see also that the relativistic contribution for the $2p_{3/2} - 2s$ transition is much smaller than for the $2p_{1/2} - 2s$ one. This is due to a large cancellation of the relativistic NMS and relativistic SMS contributions for the $2p_{3/2} - 2s$ transition. We note also that for the $2p_{1/2} - 2s$ transition the NMS equals to zero in hydrogenlike ions with a pointlike nucleus.

The total results for the MS coefficient K for the $2p_{1/2} - 2s$ and $2p_{3/2} - 2s$ transitions in Li-like ions with the nuclear charge numbers $Z = 3 - 92$ are presented in Table V. Now the leading theoretical uncertainty for middle- and high- Z ions is determined by uncalculated electron-electron interaction effects of the QED recoil contribution.

Table IV. Individual contributions to the mass shift coefficient K (1000 GHz·amu) for the $2p_{1/2} - 2s$ and $2p_{3/2} - 2s$ transitions in Li-like uranium ($Z=92$).

Subset	$2p_{1/2} - 2s$	$2p_{3/2} - 2s$	Ref.
MS operator	-733	-2010	
	-2312 ^{nr}	-2312 ^{nr}	
	-768 ^{hyd}	-2174 ^{hyd}	
NMS	-3665	-6671	
SMS	-4633	-2547	
RNMS	3892	6443	
RSMS	3673	764	
QED	-3000(32)	-2851(32)	
1-el QED	-2222	-2729	
2-el QED	-778	-122	
Total theory	-3734(32)	-4861(32)	

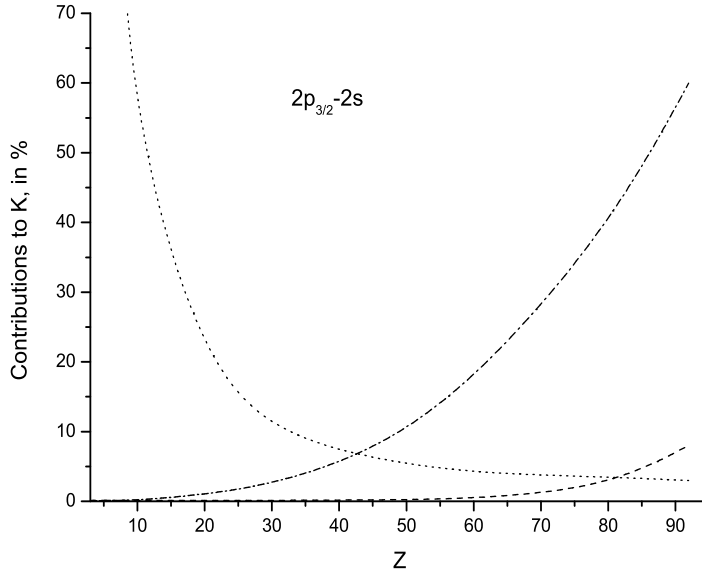
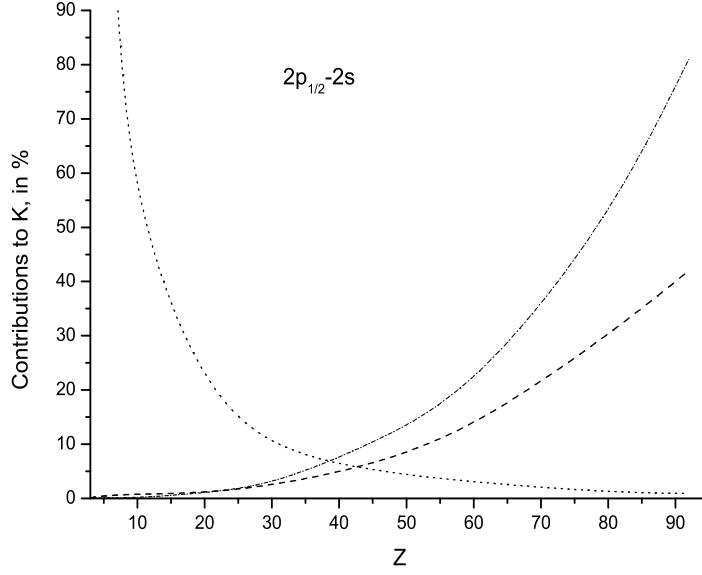


Figure 1. Relative values (in %) of the individual contributions to the mass shift coefficient K for the $2p_{1/2} - 2s$ and $2p_{3/2} - 2s$ transitions in Li-like ions. The dotted line represents the relative contribution of the electron-electron interaction; the dashed line denotes the relativistic correction; and the dashed-dotted line indicates the QED correction.

Table V. Mass shift coefficient K (GHz·amu) for the $2p_{1/2} - 2s$ and $2p_{3/2} - 2s$ transitions in Li-like ions.

Z	$2p_{1/2} - 2s$			$2p_{3/2} - 2s$		
	MS operator	QED	Total	MS operator	QED	Total
3	-443.8(2)	-0.08(3)	-443.9(2)	-443.8(2)	-0.08(3)	-443.9(2)
5	-3281.4(5)	-0.89(18)	-3282.3(5)	-3282.2(5)	-0.92(18)	-3283.1(5)
10	-20420.0(5)	-27.4(3.0)	-20447(3)	-20456.6(5)	-26.7(3.0)	-20483(3)
20	-96182(2)	-802(40)	-9698(4)×10	-97092(2)	-774(40)	-9787(4)×10
30	-22460.0(3)×10	-591(20)×10	-23051(20)×10	-23007.3(3)×10	-560(20)×10	-23568(20)×10
40	-3997.4(1)×10 ²	-251(7)×10 ²	-4248(7)×10 ²	-4194(7)×10 ²	-234.1(2)×10 ²	-4428(7)×10 ²
50	-6102.5(2)×10 ²	-796(16)×10 ²	-6899(16)×10 ²	-6643.7(2)×10 ²	-735(16)×10 ²	-7379(16)×10 ²
60	-8345.1(3)×10 ²	-2133(35)×10 ²	-10478(35)×10 ²	-9626.6(3)×10 ²	-1958(35)×10 ²	-11584(35)×10 ²
70	-1029.41(4)×10 ³	-515(7)×10 ³	-1544(7)×10 ³	-1305.85(4)×10 ³	-473(7)×10 ³	-1779(7)×10 ³
80	-1105.6×10 ³	-1167(14)×10 ³	-2272(14)×10 ³	-1669.5×10 ³	-1082(14)×10 ³	-2751(14)×10 ³
92	-733×10 ³	-3000(32)×10 ³	-3734(32)×10 ³	-2010×10 ³	-2851(32)×10 ³	-4861(32)×10 ³

III. HIGHER-ORDER ELECTRON-CORRELATION CORRECTIONS TO THE TRANSITION ENERGIES

Electron-electron interaction within the basic principles of QED is described by exchange of virtual photons. The one-photon exchange leads to the operator

$$I(\omega) = e^2 \alpha_1^\mu \alpha_2^\nu D_{\mu\nu}(\omega, \mathbf{r}_{12}), \quad (8)$$

where $D_{\mu\nu}$ is the photon propagator, which in the Coulomb gauge is written as

$$\begin{aligned} D_{00}(\omega, \mathbf{r}_{12}) &= \frac{1}{4\pi r_{12}}, \quad D_{i0} = D_{0i} = 0 \quad (i = 1, 2, 3), \\ D_{il}(\omega, \mathbf{r}_{12}) &= \int \frac{d\mathbf{k}}{(2\pi)^3} \frac{\exp(i\mathbf{k} \cdot \mathbf{r}_{12})}{\omega^2 - \mathbf{k}^2 + i0} \left(\delta_{il} - \frac{k_i k_l}{\mathbf{k}^2} \right) \quad (i, l = 1, 2, 3), \end{aligned} \quad (9)$$

$r_{12} = |\mathbf{r}_{12}| = |\mathbf{r}_1 - \mathbf{r}_2|$, \mathbf{r}_i is the position vector of the i th electron, and $\alpha^\mu = (1, \boldsymbol{\alpha})$ are the Dirac matrices.

Expanding expression (9) in powers of the photon frequency one can derive a simplified form of the interaction. The low-frequency limit of this interaction consists of two parts, referred to as the Coulomb and the Breit interaction,

$$V(i, j) = V_C(i, j) + V_B(i, j) = \frac{\alpha}{r_{ij}} - \alpha \left[\frac{\boldsymbol{\alpha}_i \cdot \boldsymbol{\alpha}_j}{2r_{ij}} + \frac{(\boldsymbol{\alpha}_i \cdot \mathbf{r}_{ij})(\boldsymbol{\alpha}_j \cdot \mathbf{r}_{ij})}{2r_{ij}^3} \right]. \quad (10)$$

The most traditional approach for the treatment of the electron-electron interaction in relativistic many-electron atoms consists in using so-called Breit approximation. In this approximation the total Hamiltonian can be represented as the sum of the one-electron Dirac Hamiltonians and the Coulomb and Breit electron-electron interactions, projected on the positive-energy Dirac's states. In this way one gets the Dirac-Coulomb-Breit equation. Traditional methods for solving the Dirac-Coulomb-Breit equation are the many-body perturbation theory (MBPT) [48, 49], the multi-configuration Dirac-Fock method [50], and the configuration-interaction (CI) method [3, 34]. All these methods treat the one-photon exchange exactly and the higher-order electron correlation is accounted for within the Breit approximation only.

The current level of experimental accuracy demands rigorous QED calculations of two-photon exchange contributions, which for $n = 2$ states of Li-like ions were performed in Refs. [6, 8–11, 13, 51]. Meanwhile rigorous QED calculations of three- and more photon exchange contributions have not been performed up to now. For high- Z few-electron ions

evaluations of these contributions within the Breit approximation are generally sufficient. Previously such calculations for Li-like ions were performed in Refs. [7, 9, 10, 13]. The evaluations of Refs. [7, 10] were carried out with the hydrogenic wave functions while in Refs. [9, 13, 52] the perturbation expansion starts with a local screening potential, which partly incorporates the electron-electron interaction effects.

In the present investigation, to evaluate the interelectronic-interaction corrections of the third and higher orders we proceed as follows. The large-scale CI-DFS method (see, e.g., Refs. [34, 38]) was used to solve the Dirac-Coulomb-Breit equation yielding the energies. The operator of the interelectronic interaction in the Breit approximation reads

$$V(\lambda) = \lambda\alpha \sum_{i>j} \left[\frac{1}{r_{ij}} - \frac{\boldsymbol{\alpha}_i \cdot \boldsymbol{\alpha}_j}{2r_{ij}} - \frac{(\boldsymbol{\alpha}_i \cdot \mathbf{r}_{ij})(\boldsymbol{\alpha}_j \cdot \mathbf{r}_{ij})}{2r_{ij}^3} \right], \quad (11)$$

where a scaling parameter λ is introduced to separate terms of different order in $1/Z$ using the numerical results obtained for different values of λ . Thus, for small λ , the total energy of the system can be expanded in powers of λ

$$E(\lambda) = E_0 + E_1\lambda + E_2\lambda^2 + \sum_{k=3}^{\infty} E_k\lambda^k, \quad (12)$$

$$E_k = \frac{1}{k!} \frac{d^k}{d\lambda^k} E(\lambda) \Big|_{\lambda=0}. \quad (13)$$

The higher-order contribution $E_{\geq 3} \equiv \sum_{k=3}^{\infty} E_k$ is calculated as

$$E_{\geq 3} = E(\lambda = 1) - E_0 - E_1 - E_2,$$

where the terms E_0 , E_1 , and E_2 are determined numerically according to Eq. (13). The results of the numerical calculation of the higher-order interelectronic-interaction contributions for the $2p_{1/2}$ - $2s$ and $2p_{3/2}$ - $2s$ transition energies in Li-like ions are collected in Table VI. ‘‘C’’ in the second column indicates that only Coulomb interaction is taken into account, while ‘‘C+B’’ means that both Coulomb and Breit interactions are included. As one can see from the table, in accordance with Refs. [7, 13], the Breit interaction contribution is rather significant, especially for middle and high- Z ions. We note that the third-order contribution monotonously increases and changes the sign when Z increases. The uncertainty of the results consists of two parts: an uncertainty due to some approximations made in the numerical procedure, in the table it is written in the first brackets, and an uncertainty due to the Breit approximation, it is given in the second brackets. To estimate the first

Table VI. The third- and higher-order interelectronic-interaction contributions to the $2p_{1/2}$ - $2s$ and $2p_{3/2}$ - $2s$ transition energies in Li-like ions, in eV. The uncertainty due to the numerical procedure is presented in the first brackets while the uncertainty due to the Breit approximation is given in the second brackets.

Z	Interaction	Contribution	$2p_{1/2} - 2s$	$2p_{3/2} - 2s$	Ref.
3	C+B	E_3	-0.4823	-0.4839	
3	C+B	$E_{\geq 3}$	-0.6483(20)(0)	-0.6499(20)(0)	
5	C+B	E_3	-0.2860	-0.2887	
5	C+B	$E_{\geq 3}$	-0.3522(15)(0)	-0.3548(15)(0)	
10	C	E_3	-0.1433	-0.1466	
10	C	$E_{\geq 3}$	-0.1583	-0.1614	
10	C+B	E_3	-0.1369	-0.1423	
10	C+B	$E_{\geq 3}$	-0.1545(6)(0)	-0.1598(6)(0)	
15	C+B	E_3	-0.0858	-0.0938	
15	C+B	$E_{\geq 3}$	-0.0942(3)(0)	-0.1025(3)(0)	
20	C+B	E_3	-0.0606	-0.0719	
20	C+B	E_3	-0.065		[53]
20	C+B	E_3	-0.069		[7]
20	C+B	$E_{\geq 3}$	-0.0635(3)(0)	-0.0747(3)(0)	
20	C+B	$E_{\geq 3}$	-0.070		[7]
30	C	E_3	-0.0406	-0.0511	
30	C	E_3	-0.045		[7]
30	C	$E_{\geq 3}$	-0.0418	-0.0518	
30	C	$E_{\geq 3}$	-0.046		[7]
30	C+B	E_3	-0.0284	-0.0470	
30	C+B	E_3	-0.0276	-0.0463	[13]
30	C+B	E_3	-0.060(8)		[51]
30	C+B	E_3	-0.030*		[51]
30	C+B	E_3	-0.036		[7]
30	C+B	$E_{\geq 3}$	-0.0296(3)(1)	-0.0481(3)(1)	
30	C+B	$E_{\geq 3}$	-0.036		[7]

Table VI. (Continued.)

Z	Interaction	Contribution	$2p_{1/2} - 2s$	$2p_{3/2} - 2s$	Ref.
35	C+B	E_3	-0.0173	-0.0401	
35	C+B	$E_{\geq 3}$	-0.0181(3)(5)	-0.0403(3)(5)	
40	C+B	E_3	-0.0070	-0.0344	
40	C+B	E_3	-0.009		[53]
40	C+B	E_3	-0.015		[7]
40	C+B	$E_{\geq 3}$	-0.0077(4)(10)	-0.0348(4)(10)	
40	C+B	$E_{\geq 3}$	-0.015		[7]
45	C+B	E_3	0.0043	-0.0286	
45	C+B	$E_{\geq 3}$	0.0017(6)(15)	-0.0314(6)(15)	
50	C	E_3	-0.0120	-0.0333	
50	C	E_3	-0.014		[53]
50	C	E_3	-0.016		[7]
50	C	$E_{\geq 3}$	-0.0133	-0.0340	
50	C+B	E_3	0.0136	-0.0271	
50	C+B	E_3	0.011		[53]
50	C+B	E_3	0.004		[7]
50	C+B	$E_{\geq 3}$	0.0113(7)(20)	-0.0283(7)(20)	
54	C+B	E_3	0.0214	-0.0250	
54	C+B	E_3	0.020		[53]
54	C+B	E_3	0.012		[7]
54	C+B	$E_{\geq 3}$	0.0195(8)(25)	-0.0260(8)(25)	
60	C+B	E_3	0.0329	-0.0236	
60	C+B	E_3	0.033		[53]
60	C+B	E_3	0.024		[7]
60	C+B	E_3	0.043		[51]
60	C+B	$E_{\geq 3}$	0.0322(10)(30)	-0.0239(10)(30)	

Table VI. (Continued.)

Z	Interaction	Contribution	$2p_{1/2} - 2s$	$2p_{3/2} - 2s$	Ref.
70	C+B	E_3	0.055	-0.025	
70	C+B	E_3	0.047		[7]
70	C+B	E_3	0.059(9)		[51]
70	C+B	E_3	0.052*		[51]
70	C+B	$E_{\geq 3}$	0.054(2)(10)	-0.024(2)(10)	
80	C+B	E_3	0.084	-0.029	
80	C+B	E_3	0.095		[53]
80	C+B	E_3	0.076		[7]
80	C+B	E_3	0.099(14)		[51]
80	C+B	E_3	0.089*		[51]
80	C+B	$E_{\geq 3}$	0.084(4)(13)	-0.028(4)(13)	
83	C	E_3	0.0328	-0.0261	
83	C	E_3	0.031		[53]
83	C	E_3	0.029		[7]
83	C	E_3	0.041	-0.024	[9]
83	C	$E_{\geq 3}$	0.0312	-0.0275	
83	C+B	E_3	0.098	-0.030	
83	C+B	E_3	0.103	-0.019	[13]
83	C+B	E_3	0.104		[53]
83	C+B	E_3	0.087		[7]
83	C+B	$E_{\geq 3}$	0.097(5)(15)	-0.029(5)(15)	
90	C+B	E_3	0.127	-0.036	
90	C+B	E_3	0.147		[53]
90	C+B	E_3	0.118		[7]
90	C+B	$E_{\geq 3}$	0.127(6)(40)	-0.035(6)(40)	

Table VI. (Continued.)

Z	Interaction	Contribution	$2p_{1/2} - 2s$	$2p_{3/2} - 2s$	Ref.
92	C+B	E_3	0.137	-0.041	
92	C+B	E_3	0.160		[53]
92	C+B	E_3	0.131		[7]
92	C+B	E_3	0.167(23)		[51]
92	C+B	E_3	0.147*		[51]
92	C+B	$E_{\geq 3}$	0.137(7)(50)	-0.039(7)(50)	

* The results of Ref. [51] with the two Breit and one Coulomb photon-exchange contributions subtracted.

uncertainty we studied the convergence of the calculation depending on the configuration basis set and compared our results with very accurate data obtained for lithium with the variational solution of the three-body Schrödinger problem that includes the relativistic corrections obtained within the αZ expansion [43, 54, 55]. The estimation of the residual three- and more photon-exchange QED effects is more difficult. As was found in Refs. [8, 13] the QED part of the two-photon exchange correction is anomalously small for the $2s$ and $2p_{1/2}$ states. Moreover, the third order of the electron-electron interaction changes its sign when Z increases. Thus, the value based on the ratio of the two-photon exchange QED correction to corresponding non-QED contribution might underestimate the three-photon QED effects. For this reason, to estimate the uncertainty due to the QED effects, we take the ratio of the QED and non-QED two-photon contributions for the $2p_{3/2} - 2s$ transition, where the QED effect is adequate, and multiply it by the maximal value of the third-order contribution among the $2s$, $2p_{1/2}$ and $2p_{3/2}$ states.

Comparing the results for the third and higher orders ($E_{\geq 3}$) with the third order (E_3), we conclude that corrections of the fourth and higher orders ($E_{\geq 3} - E_3$) are rather important, especially for low- and middle- Z ions.

We observe a reasonable agreement with Zhrebtsov *et al.* [7] and Yerokhin *et al.* [13]. A small discrepancy with the results of Yerokhin *et al.* is caused by a different way of taking into account the Breit interaction. Yerokhin *et al.* treated the Breit interaction to first order

only (exchange by only one Breit and two Coulomb photons), whereas we calculated so called “iterated” Breit interaction (exchange by two Breit and one Coulomb photons, and by three Breit photons). It should be also mentioned that Yerokhin *et al.* [13] included the negative-energy contribution for the correction considered. However, this contribution is relatively small. As comparing to Andreev *et al.* [51], a distinct deviation is found. Most probably, as indicated in Ref. [13], it is due to an overestimation of the contribution induced by two Breit and one Coulomb photon exchange in Ref. [51]. The results with this contribution subtracted are marked by an asterisk in the table. They are much closer to our results.

In Table VII we collect all the electronic-structure contributions to the transition energies and compare our results with those by other authors. For comparison we chose the most recent data from Ref. [13], which are in reasonable agreement with others calculations. Only for light ions with small $Z = 3 - 15$, where the correlation effects are large compared to the relativistic contributions, results of other works (without QED effects) are also presented. The column labeled “Dirac” contains the energy value obtained from the Dirac equation with an extended nucleus. The Fermi nuclear charge distribution was employed. Except for uranium, the root-mean-square (rms) radii were taken from Ref. [56]. In case of uranium, we use the rms value from Ref. [16] and take into account the nuclear deformation effect (see Ref. [16] for details). The two-photon exchange correction is evaluated within the framework of QED, following our previous investigations [8, 11]. The uncertainty given is due to the higher-order interelectronic interaction only. In addition to a different treatment of the Breit interaction in the present work and in Ref. [13] (see the related discussion above), we note some difference in evaluation of the QED part of the two-photon exchange contribution. In our work it was calculated with the pure Coulomb potential while in Ref. [13] a local screening potential was employed. We remind also the reader that, in accordance with our definition of the electronic-structure part, the values in Table VII are given in the nonrecoil limit.

Table VII. Electronic-structure contributions to the $2p_{1/2} - 2s$ and $2p_{3/2} - 2s$ transition energies in Li-like ions, in eV. The nuclear-charge rms radii $\langle r^2 \rangle^{1/2}$ (in fm) are taken from Refs. [16, 56]. The uncertainty given is due to the higher-order interelectronic interaction only. The first one is caused by the numerical procedure while the second one is due to the Breit approximation.

Z	$\langle r^2 \rangle^{1/2}$	Transition	Dirac	1ph	2ph	≥ 3 ph	Total	Total Ref. [13]
3	2.431	$2p_{1/2} - 2s$	0.00000	5.77750	-3.28214	-0.6484	1.8470(20)(0)	1.8466(105) 1.84812 ^a 1.8486 ^b
3	2.431	$2p_{3/2} - 2s$	0.00367	5.76900	-3.27566	-0.6499	1.8471(20)(0)	1.8466(105) 1.84816 ^a 1.8486 ^b
5	2.406	$2p_{1/2} - 2s$	0.00000	9.64178	-3.29242	-0.3522	5.9972(15)(0)	5.9963(32) 5.9986(3) ^b
5	2.406	$2p_{3/2} - 2s$	0.02832	9.60222	-3.27437	-0.3548	6.0014(15)(0)	6.0004(32) 6.0027(3) ^b
7	2.558	$2p_{1/2} - 2s$	-0.00001	13.52503	-3.30788	-0.2354	9.9817(10)(0)	9.9814(21) 9.9823(3) ^b
7	2.558	$2p_{3/2} - 2s$	0.10889	13.41639	-3.27242	-0.2391	10.0138(10)(0)	10.0133(21) 10.0144(3) ^b
10	3.005	$2p_{1/2} - 2s$	-0.00008	19.40227	-3.34105	-0.1545	15.9067(6)(0)	15.9064(10) 15.9068(3) ^b
10	3.005	$2p_{3/2} - 2s$	0.45426	19.08472	-3.26835	-0.1598	16.1108(6)(0)	16.1105(10) 16.1111(3) ^b
15	3.189	$2p_{1/2} - 2s$	-0.00046	29.40265	-3.42321	-0.0942	25.8848(3)(0)	25.8851(5) 25.8848(3) ^b
15	3.189	$2p_{3/2} - 2s$	2.30928	28.32447	-3.25801	-0.1025	27.2732(3)(0)	27.2734(5) 27.2735(3) ^b

^a Reference [55].

^b Reference [48].

Table VII. (Continued.)

Z	$\langle r^2 \rangle^{1/2}$	Transition	Dirac	1ph	2ph	≥ 3 ph	Total	Total Ref. [13]
18	3.427	$2p_{1/2} - 2s$	-0.00114	35.57028	-3.48920	-0.0738	32.0061(3)(0)	32.0060(5)
18	3.427	$2p_{3/2} - 2s$	4.80429	33.69830	-3.24944	-0.0838	35.1694(3)(0)	35.1691(5)
20	3.476	$2p_{1/2} - 2s$	-0.00185	39.76906	-3.54046	-0.0635	36.1633(3)(0)	36.1634(5)
20	3.476	$2p_{3/2} - 2s$	7.34120	37.19179	-3.24261	-0.0747	41.2157(3)(0)	41.2155(5)
21	3.544	$2p_{1/2} - 2s$	-0.00237	41.89790	-3.56830	-0.0593	38.2679(3)(0)	38.2682(5)
21	3.544	$2p_{3/2} - 2s$	8.93553	38.90849	-3.23885	-0.0712	44.5340(3)(0)	44.5339(5)
26	3.737	$2p_{1/2} - 2s$	-0.00676	52.88124	-3.73042	-0.04110	49.1030(3)(0)	49.1029(5)
26	3.737	$2p_{3/2} - 2s$	21.16322	47.14284	-3.21611	-0.0561	65.0339(3)(0)	65.0333(5)
28	3.775	$2p_{1/2} - 2s$	-0.00965	57.45499	-3.80693	-0.0353	53.6031(3)(1)	53.6034(5)
28	3.775	$2p_{3/2} - 2s$	28.57046	50.25007	-3.20517	-0.0518	75.5636(3)(1)	75.5633(5)
30	3.929	$2p_{1/2} - 2s$	-0.01434	62.14676	-3.88932	-0.0296	58.2135(3)(1)	58.2130(5)
30	3.929	$2p_{3/2} - 2s$	37.79922	53.23463	-3.19217	-0.0481	87.7936(3)(1)	87.7926(5)
36	4.188	$2p_{1/2} - 2s$	-0.03884	77.03795	-4.18113	-0.0159	72.8021(3)(5)	72.8013(6)
36	4.188	$2p_{3/2} - 2s$	79.45643	61.33404	-3.14609	-0.0390	137.6054(3)(5)	137.6044(6)
40	4.270	$2p_{1/2} - 2s$	-0.06839	87.76278	-4.41614	-0.0077	83.2706(4)(10)	83.2701(8)
40	4.270	$2p_{3/2} - 2s$	122.39809	65.89147	-3.10591	-0.0347	185.1490(4)(10)	185.1476(10)
47	4.544	$2p_{1/2} - 2s$	-0.18121	108.43093	-4.91254	0.0054	103.3426(6)(15)	103.3418(14)
47	4.544	$2p_{3/2} - 2s$	238.40726	71.83668	-3.01448	-0.0303	307.1992(6)(15)	307.1988(17)
50	4.654	$2p_{1/2} - 2s$	-0.26811	118.16524	-5.16445	0.0113	112.7440(7)(20)	112.7433(16)
50	4.654	$2p_{3/2} - 2s$	308.58586	73.43976	-2.96522	-0.0283	379.0321(7)(20)	379.0323(19)
52	4.743	$2p_{1/2} - 2s$	-0.34806	124.99085	-5.34549	0.0154	119.3127(8)(22)	119.3110(16)
52	4.743	$2p_{3/2} - 2s$	363.69747	74.14337	-2.92756	-0.0271	434.8862(8)(22)	434.8850(20)
54	4.787	$2p_{1/2} - 2s$	-0.44234	132.10903	-5.53908	0.0195	126.1471(8)(28)	126.1444(20)
54	4.787	$2p_{3/2} - 2s$	426.27988	74.52795	-2.88604	-0.0260	497.8958(8)(28)	497.8940(24)
60	4.912	$2p_{1/2} - 2s$	-0.88944	155.44266	-6.20420	0.0322	148.3812(10)(40)	148.3786(25)
60	4.912	$2p_{3/2} - 2s$	666.61398	73.51308	-2.73855	-0.0239	737.3646(10)(40)	737.3621(35)

Table VII. (Continued.)

Z	$\langle r^2 \rangle^{1/2}$	Transition	Dirac	1ph	2ph	≥ 3 ph	Total	Total Ref. [13]
70	5.311	$2p_{1/2} - 2s$	-2.91444	202.61211	-7.64776	0.0544	192.104(2)(10)	192.1023(38)
70	5.311	$2p_{3/2} - 2s$	1299.24227	62.72945	-2.38263	-0.0242	1359.565(2)(10)	1359.5629(52)
80	5.463	$2p_{1/2} - 2s$	-8.57680	264.30462	-9.68045	0.0837	246.131(4)(13)	246.130(6)
80	5.463	$2p_{3/2} - 2s$	2359.15998	36.01281	-1.82616	-0.0279	2393.319(4)(13)	2393.317(8)
83	5.521	$2p_{1/2} - 2s$	-11.89801	286.67896	-10.44836	0.0970	264.430(5)(15)	264.427(7)
83	5.521	$2p_{3/2} - 2s$	2792.20782	23.81784	-1.60493	-0.0290	2814.391(5)(15)	2814.392(9)
90	5.710	$2p_{1/2} - 2s$	-26.00449	348.27283	-12.62608	0.1270	309.769(6)(40)	309.780(10)
90	5.710	$2p_{3/2} - 2s$	4077.38297	-14.49611	-0.95621	-0.0350	4061.896(6)(40)	4061.908(11)
92	5.857	$2p_{1/2} - 2s$	-33.304	368.83426	-13.37086	0.1370	322.296(7)(50)	322.292(11)*
92	5.857	$2p_{3/2} - 2s$	4527.933	-28.41302	-0.72818	-0.0390	4498.753(7)(50)	4498.750(12)*

* Corrected for the nuclear deformation effect and the rms value from Ref. [16].

IV. SCREENED QED CORRECTIONS

The screened QED contribution ΔE_{scrQED} incorporates the screened SE ΔE_{scrSE} and screened VP ΔE_{scrVP} corrections. As concerns the QED part of the two-photon exchange correction, it is included in the electronic-structure contribution (see the previous section). Therefore, here we restrict ourself with the contributions of the screened SE and VP terms into the $2p_j - 2s$ transition energies of Li-like ions.

First estimates of the screened QED corrections in Li-like ions were performed in Refs. [1–3, 49, 50], where these corrections were included either phenomenologically or partly. The rigorous evaluations of the screened SE and VP corrections were first performed in works [4, 57] and [5], respectively. These calculations incorporate the second-order QED effects starting with the pure Coulomb potential as the zeroth-order approximation (the original Furry picture). Later, in case of Li-like bismuth, these corrections were calculated starting with a local screening potential (the extended Furry picture) [9].

In the present paper the screened SE and VP corrections are evaluated within the extended Furry representation for the ionization energies of the $2s$, $2p_{1/2}$, and $2p_{3/2}$ states of

Li-like ions in the range of the nuclear charge number $Z = 10 - 92$. Employing the extended Furry representation, one partially takes into account the higher-order electron-electron interaction effects, that are beyond the considered order of the perturbative expansion. This approach can accelerate the convergence of the QED perturbation theory with respect to the interelectronic-interaction effects, especially for small values of Z , where the convergence of the perturbative expansion becomes slower.

The Dirac equation in the extended Furry representation can be written as

$$\left[-i\boldsymbol{\alpha} \cdot \boldsymbol{\nabla} + \beta + V_{\text{nuc}} + V_{\text{scr}} \right] |n\rangle = \varepsilon_n |n\rangle, \quad (14)$$

where V_{nuc} is the Coulomb potential of the extended nucleus and V_{scr} is a local screening potential, which partially accounts for the interaction between the valence electron and the closed core electrons. We employ here the Kohn-Sham screening potential derived within the density-functional theory [58],

$$V_{\text{scr}}(r) = \alpha \int_0^\infty dr' \frac{1}{r'} \rho_t(r') - \frac{2\alpha}{3} \frac{\alpha}{r} \left(\frac{81}{32\pi^2} r \rho_t(r) \right)^{1/3}. \quad (15)$$

This potential was successfully utilized in our previous QED calculations for the g factor and hyperfine splitting of Li-like ions [59–61]. Here, ρ_t denotes the total radial charge density distribution of the core electrons (b) and the valence electron (a)

$$\rho_t(r) = \sum_b [G_b^2(r) + F_b^2(r)] + [G_a^2(r) + F_a^2(r)], \quad \int_0^\infty dr \rho_t(r) = n_b + 1, \quad (16)$$

where n_b is the number of the core electrons. The Kohn-Sham potential is constructed for the lithiumlike ground state, namely, for the $(1s^2)2s$ state. In order to estimate the sensitivity of the result on the choice of the potential we consider also the core-Hartree potential, which is just a Coulomb potential generated by the core electrons. The screening potentials are generated self-consistently by solving the Dirac equation (14) until the energies of the core and valence states become stable on the level of 10^{-9} . The asymptotic behavior of the Kohn-Sham potentials at large distances is restored by introducing the Latter correction [62].

The complete gauge invariant set of diagrams which have to be considered are shown in Fig. 2. They are referred to the SE ($a - c$) and VP ($d - f$) diagrams. The counterterm associated with the extra interaction term V_{scr} is represented graphically by the symbol \otimes . The formal expressions for these diagrams are derived from the first principles of QED employing the two-time Green-function method [63].

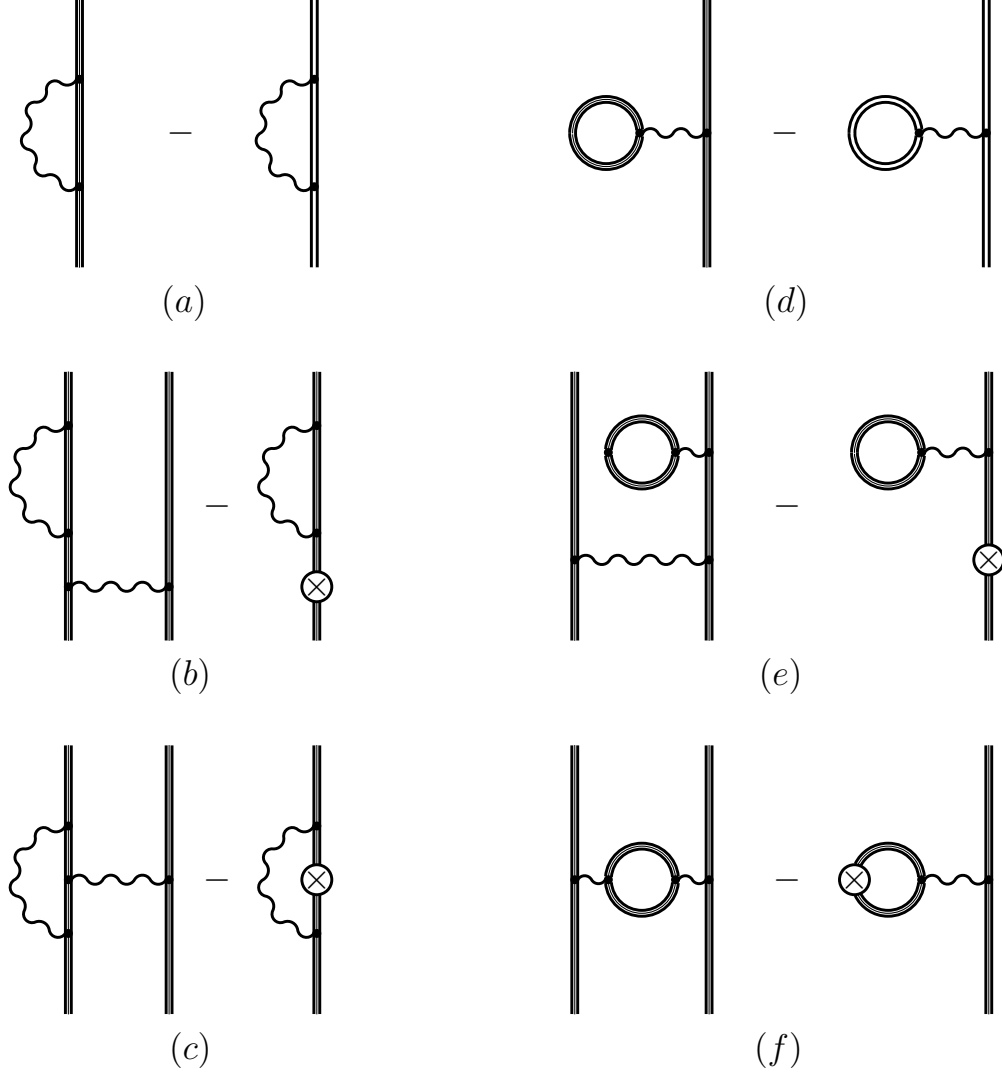


Figure 2. Feynman diagrams representing the screened SE ($a - c$) and VP ($d - f$) corrections in the extended Furry representation. The wavy line indicates the photon propagator, the triple line displays the electron propagators in the effective potential, and the double line indicates the electron propagators in the Coulomb field of the nucleus. The symbol \otimes represents the extra interaction term associated with the local screening potential.

We consider here only the diagrams contributing to the ionization energy of the valence state. It means that the one-electron core and core-core interaction diagrams are omitted in our consideration. The corresponding contribution from the SE screening diagrams can be written as

$$\Delta E_{\text{scrSE}}^{(b)a} = \Delta E_{\text{scrSE}}^{(0)} + \Delta E_{\text{scrSE}}^{(1,\text{irr})} + \Delta E_{\text{scrSE}}^{(1,\text{red})} + \Delta E_{\text{scrSE}}^{(1,\text{ver})}. \quad (17)$$

The zero-order contribution $\Delta E_{\text{scrSE}}^{(0)}$, depicted on Fig. 2(a), is the difference between the SE corrections calculated with and without the screening potential

$$\Delta E_{\text{scrSE}}^{(0)} = \langle a | \Sigma(\varepsilon_a) | a \rangle - \langle a_C | \Sigma(\varepsilon_{a_C}) | a_C \rangle. \quad (18)$$

Here, the subscript ‘‘C’’ labels the energies and wave functions calculated with the Coulomb potential of the nucleus only, while $\Sigma(\varepsilon)$ denotes the unrenormalized self-energy operator. The contribution of the diagrams depicted in Fig. 2(b) is conveniently divided into irreducible and reducible parts [63]. The irreducible part is represented by the expression

$$\begin{aligned} \Delta E_{\text{scrSE}}^{(1, \text{irr})} = & 2 \sum_b \sum_P (-1)^P \left[\sum_n^{\varepsilon_n \neq \varepsilon_a} \frac{\langle PaPb | I(\Delta) | nb \rangle \langle n | \Sigma(\varepsilon_a) | a \rangle}{\varepsilon_a - \varepsilon_n} \right. \\ & \left. + \sum_n^{\varepsilon_n \neq \varepsilon_b} \frac{\langle PaPb | I(\Delta) | an \rangle \langle n | \Sigma(\varepsilon_b) | b \rangle}{\varepsilon_b - \varepsilon_n} \right] - 2 \sum_n^{\varepsilon_n \neq \varepsilon_a} \frac{\langle a | V_{\text{scr}} | n \rangle \langle n | \Sigma(\varepsilon_a) | a \rangle}{\varepsilon_a - \varepsilon_n}, \quad (19) \end{aligned}$$

where the sum over b runs over all core electron states, P is the permutation operator, giving rise to the sign $(-1)^P$ of the permutation, $\Delta = \varepsilon_{Pa} - \varepsilon_a$, and $I(\omega)$ is the interelectronic-interaction operator defined in the Coulomb gauge by Eqs. (8) and (9). The expression for the reducible part is given by

$$\begin{aligned} \Delta E_{\text{scrSE}}^{(1, \text{red})} = & \sum_b \sum_P (-1)^P \left[\langle PaPb | I(\Delta) | ab \rangle \left(\langle a | \Sigma'(\varepsilon_a) | a \rangle + \langle b | \Sigma'(\varepsilon_b) | b \rangle \right) \right. \\ & \left. - \langle PaPb | I'(\Delta) | ab \rangle \left(\langle a | \Sigma(\varepsilon_a) | a \rangle - \langle b | \Sigma(\varepsilon_b) | b \rangle \right) \right] - \langle a | V_{\text{scr}} | a \rangle \langle a | \Sigma'(\varepsilon_a) | a \rangle. \quad (20) \end{aligned}$$

The vertex part, corresponding to Fig. 2(c), is given by

$$\begin{aligned} \Delta E_{\text{scrSE}}^{(1, \text{ver})} = & \sum_b \sum_P (-1)^P \frac{i}{2\pi} \int_{-\infty}^{\infty} d\omega \sum_{n_1, n_2} \left[\frac{\langle Pbn_1 | I(\Delta) | bn_2 \rangle \langle Pan_2 | I(\omega) | n_1 a \rangle}{(\varepsilon_{Pa} - \omega - u\varepsilon_{n_1})(\varepsilon_a - \omega - u\varepsilon_{n_2})} \right. \\ & \left. + \frac{\langle Pan_1 | I(\Delta) | an_2 \rangle \langle Pbn_2 | I(\omega) | n_1 b \rangle}{(\varepsilon_{Pb} - \omega - u\varepsilon_{n_1})(\varepsilon_b - \omega - u\varepsilon_{n_2})} \right] \\ & - \frac{i}{2\pi} \int_{-\infty}^{\infty} d\omega \sum_{n_1, n_2} \frac{\langle n_1 | V_{\text{scr}} | n_2 \rangle \langle an_2 | I(\omega) | n_1 a \rangle}{(\varepsilon_a - \omega - u\varepsilon_{n_1})(\varepsilon_a - \omega - u\varepsilon_{n_2})}, \quad (21) \end{aligned}$$

where $u = 1 - i0$ preserves the proper treatment of poles of the electron propagators. Expressions (18)-(21) suffer from ultraviolet divergences. To cancel these divergences explicitly we have employed the renormalization scheme presented in details in Refs. [4, 64]. The infrared divergences which occur in some terms of the expressions (20) and (21) are regularized by introducing a nonzero photon mass and canceled analytically.

The corresponding contributions of the screened VP diagrams, depicted in Fig. 2(d)-(f), are

$$\Delta E_{\text{scrVP}}^{(b)a} = \Delta E_{\text{scrVP}}^{(0)} + \Delta E_{\text{scrVP}}^{(1, \text{irr})} + \Delta E_{\text{scrVP}}^{(1, \text{red})} + \Delta E_{\text{scrVP}}^{(1, b)}, \quad (22)$$

$$\Delta E_{\text{scrVP}}^{(0)} = \langle a|U_{\text{VP}}|a\rangle - \langle a_{\text{C}}|U_{\text{VP}}|a_{\text{C}}\rangle, \quad (23)$$

$$\begin{aligned} \Delta E_{\text{scrVP}}^{(1, \text{irr})} = & 2 \sum_b \sum_P (-1)^P \left[\sum_n^{\varepsilon_n \neq \varepsilon_a} \frac{\langle PaPb|I(\Delta)|nb\rangle \langle n|U_{\text{VP}}|a\rangle}{\varepsilon_a - \varepsilon_n} \right. \\ & \left. + \sum_n^{\varepsilon_n \neq \varepsilon_b} \frac{\langle PaPb|I(\Delta)|an\rangle \langle n|U_{\text{VP}}|b\rangle}{\varepsilon_b - \varepsilon_n} \right] - 2 \sum_n^{\varepsilon_n \neq \varepsilon_a} \frac{\langle a|V_{\text{scr}}|n\rangle \langle n|U_{\text{VP}}|a\rangle}{\varepsilon_a - \varepsilon_n}, \end{aligned} \quad (24)$$

$$\Delta E_{\text{scrVP}}^{(1, \text{red})} = - \sum_b \sum_P (-1)^P \langle PaPb|I'(\Delta)|ab\rangle \left(\langle a|U_{\text{VP}}|a\rangle - \langle b|U_{\text{VP}}|b\rangle \right), \quad (25)$$

$$\Delta E_{\text{scrVP}}^{(1, b)} = \sum_b \sum_P (-1)^P \langle PaPb|I_{\text{VP}}(\Delta)|ab\rangle - \langle a|U_{\text{VP}}^{\text{scr}}|a\rangle, \quad (26)$$

where U_{VP} denotes the VP potential, and $I_{\text{VP}}(\Delta)$ is the interelectronic-interaction operator modified by the electron-loop. For the renormalization of the expressions (23)-(26) we refer to the works [5, 65]. Accordingly, these contributions are divided into the Uehling and Wichmann-Kroll parts. The renormalized Uehling parts of the VP operators U_{VP} and $I_{\text{VP}}(\Delta)$ are given by the expressions (see, e.g., Ref. [5])

$$\begin{aligned} U_{\text{VP}}(r) = & -\frac{2\alpha^2 Z}{3r} \int_1^\infty dt \frac{\sqrt{t^2 - 1}}{t^3} \left(1 + \frac{1}{2t^2} \right) \int_0^\infty dr' r' \rho_{\text{eff}}(r') \\ & \times [\exp(-2|r - r'|t) - \exp(-2|r + r'|t)], \end{aligned} \quad (27)$$

$$I_{\text{VP}}(\Delta, r_{12}) = \alpha \frac{\alpha_{1\mu} \alpha_2^\mu}{r_{12}} \frac{2\alpha}{3\pi} \int_1^\infty dt \frac{\sqrt{t^2 - 1}}{t^2} \left(1 + \frac{1}{2t^2} \right) \exp(-\sqrt{4t^2 - \Delta^2} r_{12}), \quad (28)$$

where the density ρ_{eff} is related to the nuclear binding and local screening potentials via the Poisson equation $\Delta V_{\text{nuc}}(r) + \Delta V_{\text{scr}}(r) = 4\pi\alpha Z \rho_{\text{eff}}(r)$. $U_{\text{VP}}^{\text{scr}}$ differs from U_{VP} only by replacing ρ_{eff} with ρ_{scr} , where the density ρ_{scr} is related to the screening potential V_{scr} . The Wichmann-Kroll parts of the expressions (23)-(25) are evaluated employing the approximate formula for the Wichmann-Kroll potential [66]. The Wichmann-Kroll contribution to Eq. (26) is relatively small [5] and is neglected in the present consideration.

The numerical evaluation is based on the wave functions constructed from B-splines employing the dual-kinetic-balance finite basis set method [67]. The sphere model for the

nuclear charge distribution is used together with the rms radii taken from Ref. [56], with the exception of the uranium ion, for which the rms value is taken from work [16]. The calculations have been performed in both Feynman and Coulomb gauges for the photon propagator describing the electron-electron interaction. The results agree very well with each other, thus providing an accurate check of the numerical procedure. In Table VIII we compare our values of the screened SE and VP corrections, calculated in the Kohn-Sham, core-Hartree, and Coulomb potentials (as zeroth-order approximation), with other theoretical results. As one can see from the table, our values for the screened SE and VP corrections in the Coulomb potential are in perfect agreement with the corresponding results of works [4, 57] and [5], respectively. As to comparison with the related values from Ref. [9], some deviation can be stated for both screened SE and VP contributions. This discrepancy is especially noticeable for the $2p_{1/2}$ and $2p_{3/2}$ screened SE terms. The reason of this disagreement is unclear for us.

In Table IX we present our results for the total screened QED correction to the ionization energies of the $2s$, $2p_{1/2}$, and $2p_{3/2}$ valence states as well as to the energy differences $2p_j - 2s$, calculated in the Kohn-Sham potential. The corresponding results obtained in the core-Hartree potential are rather close to the Kohn-Sham ones. Therefore, for the conservative estimation of the theoretical uncertainty of the ionization energies due to the higher-order contributions we consider the difference between the values obtained in the Coulomb and Kohn-Sham potentials and assign the uncertainty to be 30% of this difference. The related uncertainty for the energy differences $2p_j - 2s$ is determined to be the maximum of the error bars for the $2p_j$ and $2s$ states.

Table VIII. The contributions of the screened self-energy $\Delta E_{\text{scrSE}}^{(b)a}$ and screened vacuum-polarization $\Delta E_{\text{scrVP}}^{(b)a}$ corrections for the $2s$, $2p_{1/2}$, and $2p_{3/2}$ states of Li-like ions for different starting potentials, in eV. Comparison with the other theoretical calculations is given.

Z	Kohn-Sham		core-Hartree		Coulomb	
	$\Delta E_{\text{scrSE}}^{(b)a}$	$\Delta E_{\text{scrVP}}^{(b)a}$	$\Delta E_{\text{scrSE}}^{(b)a}$	$\Delta E_{\text{scrVP}}^{(b)a}$	$\Delta E_{\text{scrSE}}^{(b)a}$	$\Delta E_{\text{scrVP}}^{(b)a}$
$2s$ state						
20	-0.0444	0.0030	-0.0443	0.0030	-0.0462	0.0032
					-0.04624(3) ^a	0.0032 ^b
50	-0.4782	0.0587	-0.4775	0.0586	-0.4879	0.0599
					-0.4881(3) ^a	0.0599 ^b
83	-2.318	0.494	-2.315	0.494	-2.356	0.503
					-2.3553(2) ^a	0.5034(3) ^b
	-2.317 ^c	0.516 ^c	-2.311 ^c	0.523 ^c	-2.363 ^c	0.527 ^c
$2p_{1/2}$ state						
20	-0.0083	0.0007	-0.0083	0.0007	-0.0098	0.0009
					-0.00983(10) ^d	0.0009 ^b
50	-0.1240	0.0186	-0.1239	0.0186	-0.1341	0.0199
					-0.1341(3) ^d	0.0200 ^b
83	-1.069	0.244	-1.065	0.243	-1.123	0.256
					-1.1218(12) ^d	0.2564(1) ^b
	-1.120 ^c	0.268 ^c	-1.102 ^c	0.268 ^c	-1.168 ^c	0.276 ^c
$2p_{3/2}$ state						
20	-0.0126	0.0007	-0.0126	0.0007	-0.0145	0.0008
					-0.01458(3) ^a	0.0008 ^b
50	-0.1603	0.0121	-0.1603	0.0121	-0.1701	0.0129
					-0.1702(3) ^a	0.0129 ^b
83	-0.752	0.069	-0.751	0.069	-0.776	0.072
					-0.7763(6) ^a	0.0719 ^b
	-0.748 ^c	0.088 ^c	-0.737 ^c	0.087 ^c	-0.816 ^c	0.087 ^c

^a Yerokhin *et al.* [57].

^c Sapirstein and Cheng [9].

^b Artemyev *et al.* [5].

^d Yerokhin *et al.* [4].

Table IX. The screened QED contributions to the ionization energies of the $2s$, $2p_{1/2}$, and $2p_{3/2}$ states and to the energy differences $2p_{1/2} - 2s$ and $2p_{3/2} - 2s$ in Li-like ions, in eV.

Z	$\langle r^2 \rangle^{1/2}$	$2s$	$2p_{1/2}$	$2p_{3/2}$	$2p_{1/2} - 2s$	$2p_{3/2} - 2s$
10	3.005	-0.0070(2)	-0.0012(1)	-0.0017(2)	0.0058(2)	0.0053(2)
12	3.057	-0.0113(2)	-0.0019(2)	-0.0028(3)	0.0094(2)	0.0085(3)
14	3.122	-0.0168(3)	-0.0029(2)	-0.0044(3)	0.0138(3)	0.0123(3)
15	3.189	-0.0200(3)	-0.0035(3)	-0.0053(4)	0.0165(3)	0.0146(4)
18	3.427	-0.0317(4)	-0.0057(4)	-0.0089(5)	0.0260(4)	0.0228(5)
20	3.476	-0.0414(5)	-0.0076(4)	-0.0119(5)	0.0338(5)	0.0294(5)
21	3.544	-0.0467(6)	-0.0087(4)	-0.0137(5)	0.0380(6)	0.0330(6)
26	3.737	-0.0797(8)	-0.0151(7)	-0.0243(8)	0.0646(8)	0.0554(8)
28	3.775	-0.0959(9)	-0.0184(8)	-0.0296(10)	0.0775(9)	0.0662(10)
30	3.929	-0.1139(10)	-0.0221(9)	-0.0357(11)	0.0917(10)	0.0782(11)
32	4.074	-0.1339(11)	-0.0266(10)	-0.0426(12)	0.1073(11)	0.0913(12)
36	4.188	-0.1800(14)	-0.0372(13)	-0.0590(15)	0.1428(14)	0.1211(15)
40	4.270	-0.2351(17)	-0.0511(15)	-0.0790(18)	0.1840(17)	0.1561(18)
47	4.544	-0.3564(22)	-0.0856(22)	-0.1243(24)	0.2708(22)	0.2322(24)
50	4.654	-0.4195(26)	-0.1054(26)	-0.1482(27)	0.3141(26)	0.2713(27)
52	4.735	-0.4657(27)	-0.1210(28)	-0.1663(27)	0.3447(28)	0.2994(27)
54	4.787	-0.5154(30)	-0.1381(32)	-0.1851(31)	0.3773(32)	0.3303(31)
60	4.912	-0.6883(38)	-0.2042(42)	-0.2522(38)	0.4841(42)	0.4361(38)
66	5.221	-0.903(5)	-0.298(5)	-0.335(4)	0.604(5)	0.567(5)
70	5.312	-1.073(5)	-0.381(7)	-0.401(5)	0.692(7)	0.672(5)
74	5.367	-1.269(6)	-0.485(8)	-0.475(6)	0.784(8)	0.794(6)
79	5.436	-1.556(7)	-0.652(10)	-0.583(6)	0.904(10)	0.973(7)
80	5.463	-1.620(8)	-0.692(11)	-0.606(7)	0.928(11)	1.014(8)
82	5.501	-1.753(8)	-0.778(12)	-0.656(7)	0.976(12)	1.097(8)
83	5.521	-1.824(9)	-0.824(13)	-0.683(6)	1.000(13)	1.141(9)
90	5.710	-2.394(11)	-1.241(17)	-0.882(8)	1.153(17)	1.512(11)
92	5.857	-2.584(11)	-1.394(19)	-0.948(9)	1.190(19)	1.637(11)

V. $2p_j - 2s$ TRANSITION ENERGIES IN LI-LIKE IONS

In this section, we collect all theoretical contributions available for the $2p_{1/2} - 2s$ and $2p_{3/2} - 2s$ transition energies for middle- Z Li-like ions, compare them with experimental results, and discuss prospects for further improvement of the theoretical accuracy. Individual contributions to the $2p_{1/2} - 2s$ and $2p_{3/2} - 2s$ transition energies are presented in Tables X and XI, respectively. The rms radii and their uncertainties are listed in the second column of the tables. These values are taken from Ref. [56]. The uncertainty of the electronic-structure values includes an error due to the model-dependence of the nuclear charge distribution. It is conservatively estimated by comparing the results obtained within the Fermi and the homogeneously charged-sphere model. Except for neon ($Z = 10$), the electronic-structure contributions given are obtained in this work. In case of neon, we use the related result of Ref. [48], which has a higher accuracy.

Next, one should take into account the first-order one-electron QED corrections. They are determined by the SE and the VP. The SE correction is obtained by interpolating the values presented in Ref. [68] for the $2s$ and $2p_{1/2}$ states and in Ref. [69] for the $2p_{3/2}$ state. The Uehling part of the VP contribution was calculated in the present work while the Wichmann-Kroll part is taken from Ref. [70].

The next corrections, which caused the largest theoretical uncertainties for middle- Z ions [13], are the nuclear recoil and screened QED contributions. The recoil effect is considered in Sec. II, while the evaluation of the screened QED corrections is presented in Sec. IV. These calculations improve considerably the accuracy of the theoretical predictions for the $2p_j - 2s$ transition energies in middle- Z Li-like ions.

Finally, we should account for the two-loop one-electron QED effect. So-called “SEVP”, “VPVP”, and “S(VP)E” subsets were recently tabulated in Ref. [15]. The remaining two-loop SE correction (the “SESE” subset) for $n = 2$ states was accomplished only for several ions with $Z \geq 60$ [12]. In order to obtain the SESE correction for middle- Z ions we use an extrapolation procedure. For the $2s$ state, the extrapolation is performed in two steps. At first, the numerical values for the $1s$ state are obtained by interpolating the numerical results of Refs. [12, 71, 72]. Then the weighted difference $\Delta_s = 8\delta E_{2s} - \delta E_{1s}$ is achieved by using low-order terms of the αZ -expansion and extrapolating the higher-order contributions from the all-order results (see Ref. [73] and references therein). An uncertainty of 30% is assigned

to these results. For the $2p_j$ states, the correction is much smaller and, for our purpose, it is sufficient to use the αZ -expansion [73] with the boundaries for the higher-order remainder $\pm 2\alpha^2(\alpha Z)^6/(8\pi^2)$.

As one can see from the tables, the total theoretical results agree well with the experimental data. Compared to the experimental accuracy, the theoretical one is generally better, almost the same in the cases of argon ($Z = 18$) and iron ($Z = 26$), and worse for neon ($Z = 10$) and scandium ($Z = 21$, the $2p_{3/2} - 2s$ transition). For middle- Z ions, the leading theoretical uncertainties arise from the higher-order screened QED and the electronic-structure contributions. For Z greater than 40 the uncertainty due to the two-loop one-electron QED corrections becomes also considerable. We conclude that the present status of the theory and experiment for middle- Z Li-like ions provides a test of QED on a level of a few tenths of a percent.

Further improvements of the theoretical predictions can be achieved by calculating the screened QED corrections of the second order in $1/Z$ and the three-photon exchange QED corrections.

Table X. Individual contributions to the $2p_{1/2} - 2s$ transition energy in Li-like ions, in eV.

Z	$\langle r^2 \rangle^{1/2}$	Electronic structure	1-loop QED	Scr.QED	Recoil	2-loop QED	Total theory	Experiment	Ref.
10	3.005(2)	15.9068(3)	-0.0200	0.0058(2)	-0.0042	0.0000	15.8883(4)	15.8887(2)	[17]
15	3.189(2)	25.8848(3)	-0.0833	0.0165(3)	-0.0071	0.00005	25.8110(4)	25.814(3)	[74]
18	3.427(2)	32.0061(3)	-0.1569	0.0260(4)	-0.0081	0.0001	31.8673(5)	31.8664(9)	[17]
20	3.476(1)	36.1633(3)	-0.2260	0.0338(5)	-0.0100	0.0002	35.9612(6)	35.9625(25)	[75]
21	3.544(2)	38.2679(3)	-0.2673	0.0380(6)	-0.0099	0.00024	38.0289(7)	38.02(4)	[76]
26	3.737(2)	49.1030(3)	-0.5565	0.0646(8)	-0.0126	0.0007(1)	48.5991(9)	48.5982(8)	[24]
								48.5997(10)	[77]
28	3.775(1)	53.6031(3)	-0.7169	0.0775(9)	-0.0142	0.0009(1)	52.9504(10)	52.9501(11)	[78, 79]
30	3.929(1)	58.2135(3)	-0.9070	0.0917(10)	-0.0149	0.0013(2)	57.3846(10)	57.3839(30)	[80]
36	4.188(1)	72.8021(6)	-1.6859	0.1428(14)	-0.0167	0.0029(5)	71.2451(15)	71.243(8)	[81]
								71.241(11)	[82]
40	4.270(1)	83.2706(11)	-2.4107	0.1840(17)	-0.0195	0.0046(10)	81.0289(23)		
47	4.544(4)	103.3426(17)	-4.1673	0.2708(22)	-0.0233	0.0094(21)	99.4321(35)	99.438(7)	[83]
50	4.654(1)	112.7440(22)	-5.1431	0.3141(26)	-0.0238	0.0124(30)	107.9036(45)	107.911(7)	[20]
52	4.743(3)	119.3127(24)	-5.8777	0.3447(28)	-0.0243	0.0147(35)	113.770(5)		
54	4.787(5)	126.1471(31)	-6.6851	0.3773(32)	-0.0257	0.0175(40)	119.831(6)	119.820(8)	[20]
60	4.912(2)	148.3812(40)	-9.5873	0.4841(42)	-0.0305	0.0271(15)	139.275(6)		

Table XI. Individual contributions to the $2p_{3/2} - 2s$ transition energy in Li-like ions, in eV.

Z	$\langle r^2 \rangle^{1/2}$	Electronic structure	1-loop QED	Scr.QED	Recoil	2-loop QED	Total theory	Experiment	Ref.
10	3.005(2)	16.1111(3)	-0.0190	0.0053(2)	-0.0042	0.0000	16.0932(4)	16.0932(2)	[17]
15	3.189(2)	27.2732(3)	-0.0781	0.0146(4)	-0.0071	0.00004	27.2026(5)	27.206(3)	[74]
18	3.427(2)	35.1694(3)	-0.1463	0.0228(5)	-0.0082	0.0001	35.0378(6)	35.0370(12)	[17]
20	3.476(1)	41.2157(3)	-0.2100	0.0294(5)	-0.0101	0.0002	41.0251(7)	41.0286(25)	[75]
21	3.544(2)	44.5340(3)	-0.2480	0.0330(6)	-0.0100	0.0002	44.3092(7)	44.3094(2)	[25]
26	3.737(2)	65.0339(3)	-0.5119	0.0554(8)	-0.0128	0.0005(1)	64.5650(9)	64.5657(17)	[77]
28	3.775(1)	75.5636(3)	-0.6574	0.0662(10)	-0.0145	0.0008(1)	74.9586(11)	74.9602(22)	[78, 79]
30	3.929(1)	87.7936(3)	-0.8294	0.0782(11)	-0.0153	0.0011(2)	87.0282(12)	87.0302(37)	[80]
36	4.188(1)	137.6054(6)	-1.5298	0.1211(15)	-0.0173	0.0024(5)	136.1818(17)	136.202	[84]
								136.173(37)	[82]
40	4.270(1)	185.1490(11)	-2.1781	0.1561(18)	-0.0204	0.0039(10)	183.1106(23)		
47	4.544(4)	307.1992(16)	-3.7439	0.2322(24)	-0.0247	0.0081(21)	303.6709(36)	303.67(3)	[83]
50	4.654(1)	379.0321(22)	-4.6129	0.2713(27)	-0.0255	0.0107(30)	374.6757(46)		
52	4.743(3)	434.8862(24)	-5.2677	0.2994(27)	-0.0262	0.0128(35)	429.904(5)		
54	4.787(5)	497.8958(31)	-5.9880	0.3303(31)	-0.0278	0.0152(40)	492.225(6)	492.34(62)	[85]
60	4.912(2)	737.3646(40)	-8.5884	0.4361(38)	-0.0338	0.0253(20)	729.204(6)		

VI. CONCLUSION

We have presented a systematic evaluation of the relativistic nuclear recoil effect in Li-like ions. The recoil correction within the leading relativistic approximation was calculated with many-electron wave functions in order to take into account the electron correlation effect. It relies on the large-scale CI-DFS method. The higher-order relativistic recoil correction were also taken into account. The results obtained are used to evaluate the $2p_j - 2s$ transition energies. They can also be employed to get the isotope shifts in Li-like ions.

A systematic QED treatment of the electron correlation for the $2p_j - 2s$ transitions in Li-like ions was presented. The rigorous QED calculation of the one- and two-photon exchange contributions is combined with the electron correlations of third and higher orders, that have been evaluated within the Breit approximation employing the CI-DFS method. The complete gauge invariant sets of the screened one-loop QED corrections have been rigorously evaluated. Different local potentials were used as the zeroth-order approximation, namely, the Coulomb, core-Hartree, and Kohn-Sham potentials. The screened QED contributions to the ionization energies of the $2s$, $2p_{1/2}$, and $2p_{3/2}$ states as well as to the $2p_j - 2s$ transition energies are presented for Li-like ions in the range $Z = 10 - 92$.

Finally, we have compiled all available theoretical contributions to the $2p_j - 2s$ transition energies in middle- Z Li-like ions for $Z = 10 - 60$. Due to the more elaborative evaluations of the electron-electron interaction in the relativistic recoil and QED contributions we have substantially reduced the total uncertainty of the theoretical predictions. A good agreement with the experimental results has been found.

VII. ACKNOWLEDGMENTS

We thank O. Zhrebtsov for providing us with his unpublished results. Valuable communications with V. Yerokhin are gratefully acknowledged. The authors acknowledge the support by RFBR (Grant No. 07-02-00126-a), GSI, DFG (Grant No. 436RUS113/950/0-1), and by the Ministry of Education and Science of Russian Federation (Program for Development of Scientific Potential of High School, Grant No. 2.1.1/1136; Program "Scientific and pedagogical specialists for innovative Russia", Grant No. P1334). Y.S.K. acknowledges support by the Dynasty Foundation and DAAD. The work of A.N.A. is supported by the

Helmholtz Gemeinschaft and GSI under the project VH–NG–421. The work of D.A.G. is supported by the grant of the President of Russian Federation, the Saint-Petersburg Government, and the FAIR–Russia Research Center. V.M.S. acknowledges the support by the Alexander von Humboldt Foundation.

- [1] S. A. Blundell, *Phys. Rev. A* **47**, 1790 (1993).
- [2] I. Lindgren, H. Persson, S. Salomonson, and A. Ynnerman, *Phys. Rev. A* **47**, R4555 (1993).
- [3] M. H. Chen, K. T. Cheng, W. R. Johnson, and J. Sapirstein, *Phys. Rev. A* **52**, 266 (1995).
- [4] V. A. Yerokhin, A. N. Artemyev, T. Beier, G. Plunien, V. M. Shabaev, and G. Soff, *Phys. Rev. A* **60**, 3522 (1999).
- [5] A. N. Artemyev, T. Beier, G. Plunien, V. M. Shabaev, G. Soff, and V. A. Yerokhin, *Phys. Rev. A* **60**, 45 (1999).
- [6] V. A. Yerokhin, A. N. Artemyev, V. M. Shabaev, M. M. Sysak, O. M. Zhrebtsov, and G. Soff, *Phys. Rev. Lett.* **85**, 4699 (2000).
- [7] O. M. Zhrebtsov, V. M. Shabaev, and V. A. Yerokhin, *Phys. Lett. A* **277**, 227 (2000).
- [8] V. A. Yerokhin, A. N. Artemyev, V. M. Shabaev, M. M. Sysak, O. M. Zhrebtsov, and G. Soff, *Phys. Rev. A* **64**, 032109 (2001).
- [9] J. Sapirstein and K. T. Cheng, *Phys. Rev. A* **64**, 022502 (2001).
- [10] O. Y. Andreev, L. N. Labzowsky, G. Plunien, and G. Soff, *Phys. Rev. A* **64**, 042513 (2001).
- [11] A. N. Artemyev, V. M. Shabaev, M. M. Sysak, V. A. Yerokhin, T. Beier, G. Plunien, and G. Soff, *Phys. Rev. A* **67**, 062506 (2003).
- [12] V. A. Yerokhin, P. Indelicato, and V. M. Shabaev, *Phys. Rev. Lett.* **97**, 253004 (2006).
- [13] V. A. Yerokhin, A. N. Artemyev, and V. M. Shabaev, *Phys. Rev. A* **75**, 062501 (2007).
- [14] Y. S. Kozhedub, D. A. Glazov, A. N. Artemyev, N. S. Oreshkina, V. M. Shabaev, I. I. Tupitsyn, A. V. Volotka, and G. Plunien, *Phys. Rev. A* **76**, 012511 (2007).
- [15] V. A. Yerokhin, P. Indelicato, and V. M. Shabaev, *Phys. Rev. A* **77**, 062510 (2008).
- [16] Y. S. Kozhedub, O. V. Andreev, V. M. Shabaev, I. I. Tupitsyn, C. Brandau, C. Kozhuharov, G. Plunien, and T. Stöhlker, *Phys. Rev. A* **77**, 032501 (2008).
- [17] B. Edlen, *Phys. Scr.* **28**, 51 (1983).

- [18] J. Schweppe, A. Belkacem, L. Blumenfeld, N. Claytor, B. Feinberg, H. Gould, V. E. Kostroun, L. Levy, S. Misawa, J. R. Mowat, and M. H. Prior, *Phys. Rev. Lett.* **66**, 1434 (1991).
- [19] P. Beiersdorfer, A. L. Osterheld, J. H. Scofield, J. R. Crespo López-Urrutia, and K. Widmann, *Phys. Rev. Lett.* **80**, 3022 (1998).
- [20] D. Feili, P. Bosselmann, K.-H. Schartner, F. Folkmann, A. E. Livingston, E. Träbert, X. Ma, and P. H. Mokler, *Phys. Rev. A* **62**, 022501 (2000).
- [21] C. Brandau, C. Kozhuharov, A. Müller, W. Shi, S. Schippers, T. Bartsch, S. Böhm, C. Böhme, A. Hoffknecht, H. Knopp, N. Grün, W. Scheid, T. Steih, F. Bosch, B. Franzke, P. H. Mokler, F. Nolden, M. Steck, T. Stöhlker, and Z. Stachura, *Phys. Rev. Lett.* **91**, 073202 (2003).
- [22] P. Beiersdorfer, H. Chen, D. B. Thorn, and E. Träbert, *Phys. Rev. Lett.* **95**, 233003 (2005).
- [23] B. A. Bushaw, W. Nörtershäuser, G. W. F. Drake, and H.-J. Kluge, *Phys. Rev. A* **75**, 052503 (2007).
- [24] S. W. Epp, J. R. Crespo López-Urrutia, G. Brenner, V. Mäckel, P. H. Mokler, R. Treusch, M. Kuhlmann, M. V. Yurkov, J. Feldhaus, J. R. Schneider, M. Wellhöfer, M. Martins, W. Wurth, and J. Ullrich, *Phys. Rev. Lett.* **98**, 183001 (2007).
- [25] M. Lestinsky, E. Lindroth, D. A. Orlov, E. W. Schmidt, S. Schippers, S. Böhm, C. Brandau, F. Sprenger, A. S. Terekhov, A. Müller, and A. Wolf, *Phys. Rev. Lett.* **100**, 033001 (2008).
- [26] X. Zhang, N. Nakamura, C. Chen, M. Andersson, Y. Liu, and S. Ohtani, *Phys. Rev. A* **78**, 032504 (2008).
- [27] D. S. Hughes and C. Eckart, *Phys. Rev.* **36**, 694 (1930).
- [28] V. M. Shabaev, *Teor. Mat. Fiz.* **63**, 394 (1985) [*Theor. Math. Phys.* **63**, 588 (1985)].
- [29] V. M. Shabaev, *Yad. Fiz.* **47**, 107 (1988) [*Sov. J. Nucl. Phys.* **47**, 69 (1988)].
- [30] V. M. Shabaev, *Phys. Rev. A* **57**, 59 (1998).
- [31] G. S. Adkins, S. Morrison, and J. Sapirstein, *Phys. Rev. A* **76**, 042508 (2007).
- [32] C. W. P. Palmer, *J. Phys. B* **20**, 5987 (1987).
- [33] V. M. Shabaev and A. N. Artemyev, *J. Phys. B* **27**, 1307 (1994).
- [34] I. I. Tupitsyn, V. M. Shabaev, J. R. Crespo López-Urrutia, I. Draganić, R. Soria Orts, and J. Ullrich, *Phys. Rev. A* **68**, 022511 (2003).
- [35] V. A. Korol and M. G. Kozlov, *Phys. Rev. A* **76**, 022103 (2007).
- [36] A. N. Artemyev, V. M. Shabaev, and V. A. Yerokhin, *Phys. Rev. A* **52**, 1884 (1995).
- [37] A. N. Artemyev, V. M. Shabaev, and V. A. Yerokhin, *J. Phys. B* **28**, 5201 (1995).

- [38] I. I. Tupitsyn, A. V. Volotka, D. A. Glazov, V. M. Shabaev, G. Plunien, J. R. Crespo López-Urrutia, A. Lapierre, and J. Ullrich, *Phys. Rev. A* **72**, 062503 (2005).
- [39] A. Lüchow and H. Kleindienst, *Chem. Phys. Lett.* **197**, 105 (1992).
- [40] A. Lüchow and H. Kleindienst, *Int. J. Quantum Chem.* **51**, 211 (1994).
- [41] R. Barrois, H. Kleindienst, and A. Lüchow, *Int. J. Quantum Chem.* **61**, 107 (1997).
- [42] M. Godefroid, C. F. Fischer, and P. Jonsson, *J. Phys. B* **34**, 1079 (2001).
- [43] Z.-C. Yan, W. Nörtershäuser, and G. W. F. Drake, *Phys. Rev. Lett.* **100**, 243002 (2008); **100**, 249903 (2009).
- [44] M. Puchalski and K. Pachucki, *Phys. Rev. A* **78**, 052511 (2008).
- [45] J. Walls, R. Ashby, J. Clarke, B. Lu, and W. van Wijngaarden, *Eur. Phys. J. D* **22**, 159 (2003).
- [46] C. J. Sansonetti, B. Richou, R. Engleman, and L. J. Radziemski, *Phys. Rev. A* **52**, 2682 (1995).
- [47] V. M. Shabaev, A. N. Artemyev, T. Beier, G. Plunien, V. A. Yerokhin, and G. Soff, *Phys. Rev. A* **57**, 4235 (1998).
- [48] W. R. Johnson, S. A. Blundell, and J. Sapirstein, *Phys. Rev. A* **37**, 2764 (1988).
- [49] A. Ynnerman, J. James, I. Lindgren, H. Persson, and S. Salomonson, *Phys. Rev. A* **50**, 4671 (1994).
- [50] P. Indelicato and J. P. Desclaux, *Phys. Rev. A* **42**, 5139 (1990).
- [51] O. Y. Andreev, L. N. Labzowsky, G. Plunien, and G. Soff, *Phys. Rev. A* **67**, 012503 (2003).
- [52] A. N. Artemyev, V. M. Shabaev, I. I. Tupitsyn, G. Plunien, and V. A. Yerokhin, *Phys. Rev. Lett.* **98**, 173004 (2007).
- [53] O. M. Zherebtsov, private communication.
- [54] M. Puchalski and K. Pachucki, *Phys. Rev. A* **73**, 022503 (2006).
- [55] Z.-C. Yan and G. W. F. Drake, *Phys. Rev. A* **66**, 042504 (2002).
- [56] I. Angeli, *At. Data Nucl. Data Tables* **87** (2004).
- [57] V. A. Yerokhin, A. N. Artemyev, V. M. Shabaev, G. Plunien, and G. Soff, *Opt. Spectrosc.* **99**, 12 (2005).
- [58] W. Kohn and L. J. Sham, *Phys. Rev.* **140**, A1133 (1965).
- [59] D. A. Glazov, A. V. Volotka, V. M. Shabaev, I. I. Tupitsyn, and G. Plunien, *Phys. Lett. A* **357**, 330 (2006).

- [60] N. S. Oreshkina, A. V. Volotka, D. A. Glazov, I. I. Tupitsyn, V. M. Shabaev, and G. Plunien, *Opt. Spektrosk.* **102**, 889 [*Opt. Spectrosc.* **102**, 815](2007).
- [61] A. V. Volotka, D. A. Glazov, I. I. Tupitsyn, N. S. Oreshkina, G. Plunien, and V. M. Shabaev, *Phys. Rev. A* **78**, 062507 (2008).
- [62] R. Latter, *Phys. Rev.* **99**, 510 (1955).
- [63] V. M. Shabaev, *Phys. Rep.* **356**, 119 (2002).
- [64] V. A. Yerokhin and V. M. Shabaev, *Phys. Rev. A* **60**, 800 (1999).
- [65] G. Soff and P. J. Mohr, *Phys. Rev. A* **38**, 5066 (1988).
- [66] A. G. Fainshtein, N. L. Manakov, and A. A. Nekipelov, *J. Phys. B* **24**, 559 (1991).
- [67] V. M. Shabaev, I. I. Tupitsyn, V. A. Yerokhin, G. Plunien, and G. Soff, *Phys. Rev. Lett.* **93**, 130405 (2004).
- [68] T. Beier, P. J. Mohr, H. Persson, and G. Soff, *Phys. Rev. A* **58**, 954 (1998).
- [69] P. J. Mohr, *Phys. Rev. A* **46**, 4421 (1992).
- [70] T. Beier, G. Plunien, M. Greiner, and G. Soff, *J. Phys. B* **30**, 2761 (1997).
- [71] V. A. Yerokhin, P. Indelicato, and V. M. Shabaev, *Phys. Rev. A* **71**, 040101 (2005).
- [72] V. A. Yerokhin, *Phys. Rev. A* **80**, 040501 (2009).
- [73] V. A. Yerokhin, P. Indelicato, and V. M. Shabaev, *Can. J. Phys.* **85**, 253004 (2007).
- [74] W. C. Martin, R. Zalubas, and A. Musgrove, *J. Phys. Chem. Ref. Data* **14**, 751 (1985).
- [75] J. Sugar and C. Corliss, *J. Phys. Chem. Ref. Data Suppl.* **14**, No.2 (1985).
- [76] S. Suckewer, J. Cecci, S. Cohen, R. Fonck, and E. Hinnov, *Phys. Lett.* **80A**, 259 (1980).
- [77] J. Reader, J. Sugar, N. Acquista, and R. Bahr, *J. Opt. Soc. Am. B* **11**, 1930 (1994).
- [78] J. Sugar, V. Kaufman, and L. Rowan, *J. Opt. Soc. Am. B* **9**, 344 (1992).
- [79] J. Sugar, V. Kaufman, and L. Rowan, *J. Opt. Soc. Am. B* **10**, 13 (1993).
- [80] U. Staude, P. Bosselmann, R. Büttner, D. Horn, K.-H. Schartner, F. Folkmann, A. E. Livingston, T. Ludziejewski, and P. H. Mokler, *Phys. Rev. A* **58**, 3516 (1998).
- [81] S. Madzunkov, E. Lindroth, N. Eklöv, M. Tokman, A. Paál, and R. Schuch, *Phys. Rev. A* **65**, 032505 (2002).
- [82] E. Hinnov, the TFTR Operating Team, B. Denne, and the JET Operating Team, *Phys. Rev. A* **40**, 4357 (1989).
- [83] P. Bosselmann, U. Staude, D. Horn, K.-H. Schartner, F. Folkmann, A. E. Livingston, and P. H. Mokler, *Phys. Rev. A* **59**, 1874 (1999).

[84] Data available on the web site www.nist.gov.

[85] S. Martin, J. P. Buchet, M. C. Buchet-Poulizac, A. Decnis, J. Desesquelles, M. Druetta, J. P. Grandin, D. Hennecart, X. Husson, and D. Leclerc, *Europhys. Lett.* **10**, 645 (1989).